

TILTED TWO-FLUID BIANCHI TYPE I MODELS

PATRIK SANDIN ^{1*}

¹*Department of Physics, University of Karlstad,
S-651 88 Karlstad, Sweden*

November 4, 2018

Abstract

In this paper we investigate expanding Bianchi type I models with two tilted fluids with the same linear equation of state, characterized by the equation of state parameter w . Individually the fluids have non-zero energy fluxes w.r.t. the symmetry surfaces, but these cancel each other because of the Codazzi constraint. We prove that when $w = 0$ the model isotropizes to the future. Using numerical simulations and a linear analysis we also find the asymptotic states of models with $w > 0$. We find that future isotropization occurs if and only if $w \leq \frac{1}{3}$. The results are compared to similar models investigated previously where the two fluids have different equation of state parameters.

PACS numbers: 04.20.-q, 04.20.Dw, 04.20.Ha, 98.80.-k, 98.80.Bp, 98.80.Jk

*Electronic address: patrik.sandin@kau.se

1 Introduction

There have been numerous investigations of spatially homogeneous (SH) cosmological models with a perfect fluid as a matter source. In the study of these models one usually distinguish between two different scenarios: when the fluid congruence is normal to the hypersurfaces of homogeneity and when it is not. The models of the first kind are called *orthogonal* or *non-tilted*, and the second kind are called *tilted* models. The orthogonal models have been studied extensively over the past few decades (see [1] and references therein), while the tilted have received detailed investigations only more recently [2]-[11]. In investigations of tilted Bianchi models, the models of type I have been ignored since they are not compatible with any net energy flux with respect to the homogeneous hypersurfaces, something a tilted fluid will induce. However, it is possible to consider models of type I with tilted fluids if one have two or more fluids; the fluids can then all be tilted and induce energy flux individually, but the total energy flux must vanish. This was done for two tilted perfect fluids with linear equations of state in [12]. The fluids had equations of state $p_{(1)} = w_{(1)} \rho_{(1)}$ and $p_{(2)} = w_{(2)} \rho_{(2)}$, where $\rho_{(i)}$ and $p_{(i)}$ are the energy densities and pressures of the respective fluids in their own rest frames, and where it was assumed that $0 \leq w_{(2)} < w_{(1)} < 1$. The case $w_{(1)} = w_{(2)}$ was left due to lack of space and because of its qualitatively different behavior – this will be the topic of the present paper.

As an example of a model with two different perfect fluids with the same equation of state one can imagine a universe filled with two kinds of dust (the pressure of both fluids is zero). This is a reasonable model for both the baryonic and cold dark matter components of the total matter content of the universe today according to observations. The study of Bianchi type I models with two tilted fluids with the same equation of state can be viewed as the simplest anisotropic tilted model generalizing the standard isotropic cosmological scenario close to flatness.

The SH Bianchi models admit a three dimensional group of isometries acting simply transitively on the spacelike hypersurfaces that define the surfaces of homogeneity. The models are classified by the Lie algebra of the isometry group, which results in a hierarchy of models of different complexity where the Bianchi type I model can be found on the bottom, its algebra being Abelian and obtainable from all the other Bianchi models by Lie algebra contractions [1]. When the Einstein field equations are formulated as a dynamical system the Bianchi type I models appear as a boundary of a larger state space describing the other Bianchi models. Describing the dynamics of this boundary is an important first step to understanding the dynamics of the more general models.

The Bianchi models are sometimes interesting even when studying general inhomogeneous cosmological models. This is the case for example in the very early universe near an initial singularity where horizons form and asymptotically shrink towards the singularity which result in the equations asymptotically approaching those of homogenous models, something referred to as *asymptotic silence* and *locality* [13].

In this paper we analyze the system of autonomous DEs derived in [12] describing the time evolution of the spatially homogeneous Bianchi type I models with two perfect fluids, but in contrast to [12] we study the case when the two equations of state are the same. The paper is organized as follows: In section 2 the system of equations and constraints is derived. In section 3 the future evolution of dust models is described, and in section 4 the evolution of models with other equation of state is investigated. Section 5 consists of a summary of the results and a discussion of their implication. Appendix A contains a description of the equilibrium points of the system and their stability properties, and appendix B studies the dynamics on the vacuum subset.

2 The dynamical system

We begin by deriving the evolution equations for the tilted two-fluid Bianchi type I models. We first give the evolution equations of a general Bianchi model, in terms of expansion-normalized variables defined relative to the timelike congruence normal to the group orbits. This derivation is described in [1], or [14], but for completeness we give a short description of it here.

First one introduces a group-invariant orthonormal frame $\{\mathbf{e}_0, \mathbf{e}_\alpha\}$, where $\mathbf{e}_0 = \mathbf{n}$ is the normal to the group orbits and $\alpha = 1, 2, 3$. The commutation functions, $\gamma^a_{bc}(t)$ are the basic variables:

$$[\mathbf{e}_b, \mathbf{e}_c] = \gamma^a_{bc} \mathbf{e}_a.$$

The commutator functions are normally decomposed according to

$$[\mathbf{e}_0, \mathbf{e}_\alpha] = -[H \delta_\alpha^\beta + \sigma_\alpha^\beta + \epsilon_\alpha^\beta{}_\gamma \Omega^\gamma] \mathbf{e}_\beta, \quad (1a)$$

$$[\mathbf{e}_\alpha, \mathbf{e}_\beta] = c^\gamma{}_{\alpha\beta} \mathbf{e}_\gamma = 2a_{[\alpha} \delta_{\beta]}{}^\gamma + \epsilon_{\alpha\beta\delta} n^{\delta\gamma}. \quad (1b)$$

where H is the Hubble scalar, which is related to the expansion θ of the normal congruence \mathbf{n} according to $H = \frac{1}{3}\theta$; $\sigma_{\alpha\beta}$ is the shear associated with \mathbf{n} ; Ω^α is the Fermi rotation which describes how the spatial triad rotates with respect to a gyroscopically fixed so-called Fermi frame; $n^{\alpha\beta}$ and a_α describe the Lie algebra of the 3-dimensional simply transitive Lie group and determine the spatial three-curvature, see e.g. [1].

The energy-momentum tensor is similarly decomposed,

$$T_{ab} = \rho n_a n_b + 2q_{(a} n_{b)} + p(g_{ab} + n_a n_b) + \pi_{ab}, \quad (2)$$

and is described by the source terms relative to the orthonormal frame,

$$\{\rho, p, q_\alpha, \pi_{\alpha\beta}\}.$$

To obtain a regular, dimensionless system of equations the commutation functions and the source terms are normalized with the hubble scalar according to

$$\begin{aligned} \Sigma_{\alpha\beta} &= \frac{\sigma_{\alpha\beta}}{H}, \quad N_{\alpha\beta} = \frac{n_{\alpha\beta}}{H}, \quad A_\alpha = \frac{a_\alpha}{H}, \quad R_\alpha = \frac{\Omega_\alpha}{H}, \\ \Omega &= \frac{\rho}{3H^2}, \quad P = \frac{p}{3H^2}, \quad Q_\alpha = \frac{q_\alpha}{3H^2}, \quad \Pi_{\alpha\beta} = \frac{\pi_{\alpha\beta}}{3H^2}. \end{aligned} \quad (3)$$

We also choose a new dimensionless time coordinate τ according to

$$\frac{d\tau}{dt} = H. \quad (4)$$

The evolution of H is determined by the deceleration parameter q ,

$$H' = -(1 + q)H, \quad (5)$$

where $'$ denotes differentiation with respect to τ . Raychaudhuri's equation gives an expression for q in terms of the variables (3):

$$q = 2\Sigma^2 + \frac{1}{2}(\Omega + 3P), \quad (6)$$

where $\Sigma^2 = \frac{1}{6}\Sigma_{\alpha\beta}\Sigma^{\alpha\beta}$. The Einstein field equations and the Jacobi identities then yields the following system of equations:

Evolution equations:

$$\Sigma'_{\alpha\beta} = -(2 - q)\Sigma_{\alpha\beta} + 2\epsilon^{\gamma\delta}{}_{\langle\alpha}\Sigma_{\beta\rangle\delta}R_\gamma - {}^3\mathcal{R}_{\langle\alpha\beta\rangle} + 3\Pi_{\alpha\beta}, \quad (7a)$$

$$A'_\alpha = [q\delta_\alpha^\beta - \Sigma_\alpha^\beta - \epsilon_\alpha^\beta{}_\gamma R^\gamma]A_\beta, \quad (7b)$$

$$(N^{\alpha\beta})' = [q\delta_\gamma^{(\alpha} + 2\Sigma_\gamma^{(\alpha} + 2\epsilon_\gamma^{(\alpha}{}_\delta R^{\delta)}]N^{\beta)\gamma}. \quad (7c)$$

Constraint equations:

$$0 = 1 - \Sigma^2 + \frac{1}{6}{}^3\mathcal{R} - \Omega, \quad (8a)$$

$$0 = (3\delta_\alpha^\gamma A_\beta + \epsilon_\alpha^{\delta\gamma} N_{\delta\beta})\Sigma^\beta{}_\gamma - 3Q_\alpha, \quad (8b)$$

$$0 = A_\beta N^\beta{}_\alpha. \quad (8c)$$

where ${}^3\mathcal{R}_{\langle\alpha\beta\rangle}$ and ${}^3\mathcal{R}$ are the trace-free and scalar parts of the Hubble-normalized three-curvature, respectively, according to:

$${}^3\mathcal{R}_{\langle\alpha\beta\rangle} = B_{\langle\alpha\beta\rangle} + 2\epsilon^{\gamma\delta}{}_{\langle\alpha} N_{\beta\rangle\delta} A_{\gamma}, \quad {}^3\mathcal{R} = -\frac{1}{2}B^\alpha{}_\alpha - 6A_\alpha A^\alpha; \quad B_{\alpha\beta} = 2N_{\alpha\gamma} N^\gamma{}_\beta - N^\gamma{}_\gamma N_{\alpha\beta},$$

and where $\langle.. \rangle$ denotes trace-free symmetrization of the indices, i.e. $A_{\langle\alpha\beta\rangle} = A_{(\alpha\beta)} - \frac{1}{3}\delta_{\alpha\beta}A_\alpha A^\beta$. The contracted Bianchi identities yields evolution equations for the total source variables:

$$\Omega' = (2q - 1)\Omega - 3P + 2A_\alpha Q^\alpha - \Sigma_{\alpha\beta}\Pi^{\alpha\beta}, \quad (9a)$$

$$Q'_\alpha = -[2(1 - q)\delta_\alpha{}^\beta + \Sigma_\alpha{}^\beta + \epsilon_\alpha{}^\beta{}_\gamma R^\gamma]Q_\beta + (3\delta_\alpha{}^\gamma A_\beta + \epsilon_\alpha{}^{\delta\gamma} N_{\delta\beta})\Pi^\beta{}_\gamma. \quad (9b)$$

These equations are a consequence of the evolution and constraint equations (7) and (8) and give no additional information, but are useful as auxiliary equations.

The system of equations (7) and (8) with (6) is not fully determined, there are no evolution equations for the variables R_α that represent the angular velocity of the spatial frame $\{\mathbf{e}_\alpha\}$. We can freely specify R_α in any way most convenient. Also the evolution of the source variables P and $\Pi_{\alpha\beta}$ are not determined until we specify a source. We consider the source to be two tilted perfect fluids, only interacting with each other gravitationally. We can then split the energy-momentum tensor into two parts, each satisfying the conservation equation separately

$$T^{ab} = \sum_i T^{ab}_{(i)}, \quad \nabla_a T^{ab}_{(i)} = 0, \quad (i = 1, 2), \quad (10)$$

where

$$T^{ab}_{(i)} = (\tilde{\rho}_{(i)} + \tilde{p}_{(i)})\tilde{u}^a_{(i)}\tilde{u}^b_{(i)} + \tilde{p}_{(i)}g^{ab}. \quad (11)$$

We now impose the same linear equation of state for the two fluids, i.e., $\tilde{p}_{(i)} = w\tilde{\rho}_{(i)}$, where $w = \text{const}$. The four velocities $\mathbf{u}_{(i)}$ can be written in the form

$$\tilde{u}^a_{(i)} = \frac{1}{\sqrt{1 - v_{a(i)}v^a_{(i)}}}(n^a + v^a_{(i)}); \quad n_a v^a_{(i)} = 0. \quad (12)$$

Since we have two separate conservation equations we now have two sets of source variables

$$\{\Omega_{(i)}, P_{(i)}, Q^{(i)}_\alpha, \Pi^{(i)}_{\alpha\beta}\}, \quad (i = 1, 2),$$

where each $\Omega_{(i)}$ and $Q^{(i)}_\alpha$ satisfies equations (9). The source variables can all be expressed in terms of the normalized energy density and the three-velocity of the respective fluid as

$$Q^{(i)}_\alpha = (1 + w)(G^{(i)}_+)^{-1} v^{(i)}_\alpha \Omega_{(i)}, \quad (13a)$$

$$P_{(i)} = w\Omega_{(i)} + \frac{1}{3}(1 - 3w)Q^{(i)}_\alpha v^{(i)\alpha}, \quad (13b)$$

$$\Pi^{(i)}_{\alpha\beta} = Q^{(i)}_{\langle\alpha} v^{(i)}_{\beta\rangle}, \quad (13c)$$

where $G^{(i)}_\pm = 1 \pm w v^2_{(i)}$ and $v^2_{(i)} = v_{\alpha(i)}v^\alpha_{(i)}$. One can use equations (9) and (13) to obtain evolution equations for the source terms $\Omega_{(i)}$ and $v^{(i)}_\alpha$:

$$\Omega'_{(i)} = (2q - 1 - 3w)\Omega_{(i)} + [(3w - 1)v_{(i)\alpha} - \Sigma_{\alpha\beta}v^\beta_{(i)} + 2A_\alpha]Q^\alpha_{(i)}, \quad (14a)$$

$$v'_{\alpha(i)} = (G^{(i)}_-)^{-1} \left[(1 - v^2_{(i)})(3w - 1 - wA^\beta v_{\beta(i)}) + (1 - w)(A^\beta + \Sigma_\gamma{}^\beta v^\gamma_{(i)})v_{\beta(i)} \right] v_{\alpha(i)} \\ - [\Sigma_\alpha{}^\beta + \epsilon_\alpha{}^{\beta\gamma}(R_\gamma + N_\gamma{}^\delta v_{\delta(i)})]v_{\beta(i)} - A_\alpha v^2_{(i)}. \quad (14b)$$

For the Bianchi type I models we have $A_\alpha = N_{\alpha\beta} = 0$. The Codazzi constraint (8b) then becomes, $Q_\alpha = Q^{(1)}_\alpha + Q^{(2)}_\alpha = 0$, which, taken in combination with (13), forces the 3-velocities of the two fluids to be anti-parallel. Kinematically the situation is similar to that of Bianchi type I with a general magnetic field studied in [15], and it is therefore natural to exploit the same mathematical structures in the present

problem. We therefore choose the spatial triad so that one of the frame vectors is aligned with the fluid velocities, which we choose to be \mathbf{e}_3 , i.e. $v_{(i)}^\alpha = (0, 0, v_{(i)})$. Demanding that these conditions on $v_{(i)}^\alpha$ hold for all times lead to the following conditions

$$R_1 = -\Sigma_{23}, \quad R_2 = \Sigma_{31}. \quad (15)$$

This leaves R_3 undetermined, however, we still have the freedom of arbitrary rotations in the 1-2-plane, which we use to set

$$R_3 = 0. \quad (16)$$

Following [15], we introduce the variables $\Sigma_+, \Sigma_A, \Sigma_B, \Sigma_C$ according to

$$\Sigma_+ = \frac{1}{2}(\Sigma_{11} + \Sigma_{22}), \quad \Sigma_{31} + i\Sigma_{23} = \sqrt{3}\Sigma_A e^{i\phi}, \quad \Sigma_- + \frac{i}{\sqrt{3}}\Sigma_{12} = (\Sigma_B + i\Sigma_C)e^{2i\phi}, \quad (17)$$

where $\Sigma_- = (\Sigma_{11} - \Sigma_{22})/(2\sqrt{3})$, which leads to

$$\Sigma^2 = \Sigma_+^2 + \Sigma_A^2 + \Sigma_B^2 + \Sigma_C^2. \quad (18)$$

The angular variable ϕ decouples from the other equations, $\phi' = -\Sigma_C$, which reduces the dimension of the dynamical system by one. The resulting dynamical system is the following:

Evolution equations:

$$\Sigma'_+ = -(2-q)\Sigma_+ + 3\Sigma_A^2 - Q_{(1)}v_{(1)} - Q_{(2)}v_{(2)}, \quad (19a)$$

$$\Sigma'_A = -(2-q + 3\Sigma_+ + \sqrt{3}\Sigma_B)\Sigma_A, \quad (19b)$$

$$\Sigma'_B = -(2-q)\Sigma_B + \sqrt{3}\Sigma_A^2 - 2\sqrt{3}\Sigma_C^2, \quad (19c)$$

$$\Sigma'_C = -(2-q - 2\sqrt{3}\Sigma_B)\Sigma_C, \quad (19d)$$

$$v'_{(i)} = (G_{-}^{(i)})^{-1}(1 - v_{(i)}^2)(3w_{(i)} - 1 + 2\Sigma_+)v_{(i)}, \quad (19e)$$

$$\Omega'_{(i)} = (2q - 1 - 3w_{(i)})\Omega_{(i)} + (3w_{(i)} - 1 + 2\Sigma_+)Q_{(i)}v_{(i)}. \quad (19f)$$

Constraint equations:

$$0 = 1 - \Sigma^2 - \Omega_{(1)} - \Omega_{(2)}, \quad (20a)$$

$$0 = Q_{(1)} + Q_{(2)}, \quad (20b)$$

where

$$q = 2\Sigma^2 + \frac{1}{2}(\Omega_m + 3P_m) = 2 - \frac{3}{2}(\Omega_m - P_m); \quad \Omega_m = \Omega_{(1)} + \Omega_{(2)}, \quad P_m = P_{(1)} + P_{(2)}. \quad (21)$$

The assumption of non-negative energy densities, $\Omega_{(i)} \geq 0$, together with (21) and (20a), yields that $\frac{1}{2} \leq q \leq 2$.

2.1 The state space

The state space consists of $\mathbf{S} = \{\Sigma_+, \Sigma_A, \Sigma_B, \Sigma_C, v_{(1)}, v_{(2)}, \Omega_{(1)}, \Omega_{(2)}\}$ subject to the constraints (20a), (20b). Both $v_{(i)} = 0$ and $v_{(i)}^2 = 1$ defines invariant subsets which means that $v_{(i)}^2$, contained in the range $(0, 1)$, is bounded both from above and below. The constraint (20a) together with the non-negativity condition on the energy densities puts bounds on all the other variables and hence the state space is bounded. We are primarily interested in the interior state space where

$$0 < \Omega_{(1)}\Omega_{(2)}, \quad 0 < v_{(i)}^2 < 1, \quad (22)$$

but asymptotically the orbits of the system may approach the boundary and hence we consider its closure, $\bar{\mathbf{S}}$, which means that we consider the set defined by $\Sigma^2 \leq 1, 0 \leq v_{(i)}^2 \leq 1; 0 \leq \Omega_{(i)} \leq 1$, in such a way that the constraints (20) are satisfied.

The dynamical system have the following discrete symmetries:

$$\Sigma_A \rightarrow -\Sigma_A, \quad \Sigma_C \rightarrow -\Sigma_C; \quad (v_{(1)}, v_{(2)}) \rightarrow -(v_{(1)}, v_{(2)}). \quad (23)$$

We therefore assume without loss of generality that $\Sigma_A \in [0, 1]$, $\Sigma_C \in [0, 1]$, $v_{(1)} \in [0, 1]$, and $v_{(2)} \in [-1, 0]$; the solutions in the other sectors of the state space are easily obtained by means of the discrete symmetries.

In [12] one had two monotone functions which here become constants of motion. Only one of them is independent of the Codazzi constraint, however, and can be written as

$$\frac{v_{(1)}^2(1 - v_{(2)}^2)^{(1-w)}}{v_{(2)}^2(1 - v_{(1)}^2)^{(1-w)}} = k. \quad (24)$$

where k is a positive real constant. The submanifolds defined by (24) foliates the state space and are dependent on w . Projections onto $v_{(1)} \times v_{(2)}$ -space for dust and almost stiff equations of state are shown in Figure 1.

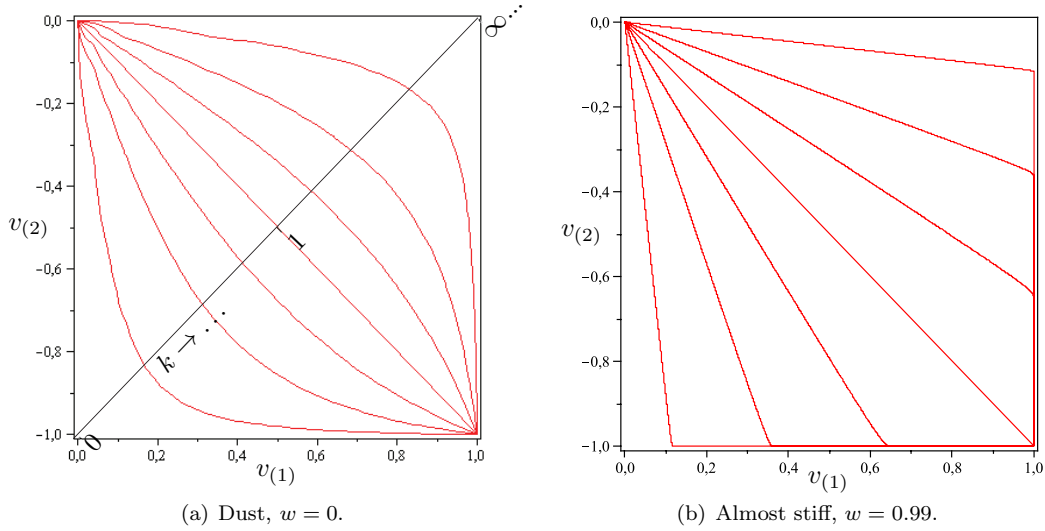


Figure 1: The leaves of foliation in $v_{(1)} \times v_{(2)}$ -space.

The constant of motion (24) correlates the velocities of the fluids such that if one of them becomes extremely tilted or orthogonal asymptotically so must the other. Note also that it is not possible that one of the fluids will dominate over the other asymptotically; if the normalized energy density of one of them vanishes then this is also the case for the other, which follows from considering the constraints (24) and (20b) simultaneously. This excludes a large part of the boundary of $\bar{\mathbf{S}}$ from consideration since it may not be approached. When examining invariant subsets and fix points on the boundary in the following we will only consider those that can be approached from the interior, i.e. not those where $\Omega_{(i)} = 0 \neq \Omega_{(j)}$, $v_{(i)} = 0 \neq v_{(j)}$, or $v_{(i)}^2 = 1 \neq v_{(j)}^2$, where $i \neq j$.

2.2 Invariant subsets

The dynamical system (19), (20), admits a number of invariant subsets, conveniently divided into two classes: (i) ‘geometric subsets’, i.e., sets associated with conditions on the shear and hence the metric; (ii) invariant sets associated with conditions on the tilt or energy densities. We will introduce a notation where the kernel suggests the type of subset and where a subscript, when existent, suggests the values of $v_{(1)}$ and $v_{(2)}$.

Geometric subsets

- \mathcal{TW} : The ‘twisting’ subset, characterized by $\Sigma_C = 0$, $\Sigma_A \neq 0$, which leads to that the decoupled ϕ -variable satisfies $\phi = \text{const}$ and hence $\Sigma_{12} \propto \Sigma_{11} - \Sigma_{22}$.

Name	$0 \leq w < \frac{1}{3}$	$\frac{1}{3} < w < \frac{1}{2}$	$\frac{1}{2} < w < \frac{5}{9}$	$\frac{5}{9}$	$\frac{5}{9} < w < 1$
K_{00}°	source/saddle				
K_{11}°	source/saddle				
$KS_{v_{(1)}v_{(2)}}^\pm$	center-saddle				
$F_{00}^{\Omega_{(1)}\Omega_{(2)}}$	sink	saddle			
$LRSL_{v_{(1)}v_{(2)}}$	does not exist	sink	saddle		
TW_{11}	saddle				
$TWL_{v_{(1)}v_{(2)}}$	does not exist		sink	$(TWL_{v_{(1)}v_{(2)}} \subset GS_{v_{(1)}v_{(2)}})$ sink $(G_{11} \subset GS_{v_{(1)}v_{(2)}})$	saddle
$GS_{v_{(1)}v_{(2)}}$	does not exist				does not exist
G_{11}	saddle				sink

Table 1: A list of fix points when $0 \leq w < 1$. The fix points are denoted by a kernel that is related to a subset of which the fix point belong in combination with a subscript and sometimes also a superscript. The subscript indicates the fix point values of $v_{(1)}$ and $v_{(2)}$. The superscript of the Friedmann fix points F_{00}^{**} indicates of the values of $\Omega_{(1)}$ and $\Omega_{(2)}$ while it denotes the sign of Σ_B in the case of the Kasner surface KS_{**}^\pm . A complete characterization of the fix points is given in Appendix A; here we have given a description in terms of their stability properties.

- \mathcal{RD} : The constantly rotated diagonal subset, given by $\Sigma_A = 0, \Sigma_C \neq 0$ ($R_\alpha = 0$). This subset is the diagonal subset, discussed next, rotated with a constant angle around e_3 .
- \mathcal{D} : The diagonal subset, defined by $\Sigma_A = \Sigma_C = 0; \Sigma_B = \Sigma_-$, and hence $R_\alpha = 0$.
- \mathcal{LRS} : The locally rotationally symmetric subset. This plane symmetric subset of the diagonal subset is characterized by the additional condition $\Sigma_B = \Sigma_- = 0$. This is the simplest subset compatible with two tilted fluids.

Matter subsets

- \mathcal{O} : The orthogonal subset for which $v_{(1)} = v_{(2)} = 0$. In this subset $\Omega_{(1)} \propto \Omega_{(2)}$ and the distinction between the two fluids becomes artificial. The orthogonal subset describes a single orthogonal fluid. In general this subset is expressed in a non-Fermi frame for which $\Sigma_A \Sigma_C \neq 0$, however, usually when dealing with this case one makes a rotation to a Fermi frame in which the shear and the metric are diagonal so that \mathcal{O} belongs to \mathcal{D} .
- \mathcal{ET}_{11} : The double extreme tilt subset where both fluids propagate with the speed of light, $v_{(1)} = 1 = -v_{(2)} \Rightarrow \Omega_{(1)} = \Omega_{(2)} = 3P_{(1)} = 3P_{(2)}$.
- \mathcal{K} : The vacuum subset is called the Kasner subset and is defined by $\Omega_m = 0; \Sigma^2 = 1$; it describes the Kasner solutions, but in general in a non-Fermi propagated frame, and with $v_{(i)}$ as test fields.

Other invariant subsets can be obtained by taking intersections of the ones described above.

Apart from the above subsets there are also a number of fix points. These, and their eigenvalues, are given in Appendix A, but we summarize them in Table 1 along with their stability properties. If $\Omega_{(1)}$ and $\Omega_{(2)}$ are zero then $v_{(1)}$ and $v_{(2)}$ act as test fields. This is the case for the Kasner fix points K_{**} which all describe the same Kasner solutions; the $KS_{v_{(1)}v_{(2)}}^\pm$ describe a particular Kasner solution determined by w ; the line of Friedmann fix points $F_{00}^{\Omega_{(1)}\Omega_{(2)}}$ describe the flat Friedmann-Lemaître solution for a single orthogonal perfect fluid with a linear equation of state. However, all the remaining fix points are physically distinct.

3 Future isotropization of tilted multi-fluid dust models

Arguably the most physically relevant equation of state is the case when $w = 0$. This describes two perfect fluids with zero pressure, commonly referred to as *dust*, and is a good description of the actual matter content of the universe during the matter dominated epoch. For this case we can prove the following proposition

Proposition 3.1. *If $w=0$, then the future asymptotic state of the system (19) is the Friedmann-Lematre solution.*

Proof. For $w = 0$ we have

$$[\ln(1 - v_{(i)}^2)\Omega_{(i)}^2]' = 2(2q - 1), \quad (25)$$

which is a monotonically increasing function since $q \geq \frac{1}{2}$. Since it is also bounded from above it must approach a limit value and hence we have $q \rightarrow \frac{1}{2}$. This implies $P_m \rightarrow 0$, $\Omega_m \rightarrow 1$, which in turn implies $v_{(i)} \rightarrow 0$. The constraint (20a) ensures isotropization and we have reduced the system to the fix points $\text{FL}_{00}^{\Omega_{(1)}\Omega_{(2)}}$. \square

Observations of galaxies and galaxy clusters correlates the distribution of dark matter with the baryonic matter visible in the galaxies, which implies that the velocity of dark matter is aligned with the velocity of visible matter [16]. The Bianchi type I model is an example of how a universe where the dust flows initially are non-aligned can evolve into a state where they become aligned asymptotically to the future.

The linear analysis of appendix A, and the dynamics on the Kasner subset, described in Appendix B and numerical simulations suggests that asymptotically to the past the system approaches a doubly extremely tilted Kasner model described by one of the fix points in (44a), as conjectured in section 4.2.

4 Future and past dynamics of general linear equations of state

4.1 Future dynamics

As was shown in [12] no tilted two-fluid Bianchi type I models with $Q_{(i)} > 0$, $v_{(i)}^2 < 1$ and $w > \frac{1}{3}$ isotropize to the future. The theorem does not tell us what the asymptotic state is other than that it is anisotropic. The conclusions we make about the future global attractors for $w < \frac{1}{3}$ rests on the local stability analysis of the fix points and numerical simulations, which makes us confident of the following conjectures:

Conjecture 4.1. *The ω -limit for all orbits that have $\Sigma_A, \Sigma_C \neq 0$ initially is contained in the set $\text{FL}_{00}^{\Omega_{(1)}\Omega_{(2)}}$ if $w \leq \frac{1}{3}$, $\text{LRSL}_{v_{(1)}v_{(2)}}$ if $\frac{1}{3} < w \leq \frac{1}{2}$, $\text{TWL}_{v_{(1)}v_{(2)}}$ if $\frac{1}{2} < w < \frac{5}{9}$, $\text{GS}_{v_{(1)}v_{(2)}}$ if $w = \frac{5}{9}$, and G_{11} if $\frac{5}{9} < w < 1$.*

Conjecture 4.2. *The ω -limit for all orbits that have $\Sigma_A \neq 0$, $\Sigma_C = 0$ initially is contained in the set $\text{FL}_{00}^{\Omega_{(1)}\Omega_{(2)}}$ if $w \leq \frac{1}{3}$, $\text{LRSL}_{v_{(1)}v_{(2)}}$ if $\frac{1}{3} < w \leq \frac{1}{2}$, $\text{TWL}_{v_{(1)}v_{(2)}}$ if $\frac{1}{2} < w < \frac{3}{5}$, and TW_{11} if $\frac{3}{5} \leq w < 1$.*

Conjecture 4.3. *The ω -limit for all orbits that have $\Sigma_A = 0$ initially is contained in the set $\text{FL}_{00}^{\Omega_{(1)}\Omega_{(2)}}$ if $w \leq \frac{1}{3}$ and in the set $\text{LRSL}_{v_{(1)}v_{(2)}}$ if $\frac{1}{3} < w < 1$.*

The conjectures about the future attractors can conveniently be summarized by three diagrams showing the attractors for different values of w , for the general Bianchi type I set, the 'twisting' subset and the diagonal subset. See figure 2.

4.2 Past dynamics

Numerical calculations, the local analysis of the fix points in appendix A, and the dynamics on the Kasner subset described in Appendix B, supports the following conjecture:

Conjecture 4.4. *The α -limit for every orbit with $Q_{(1)} > 0$, $v_{(1)}^2 < 1$, $v_{(2)}^2 < 1$ initially on the general geometric set with $\Sigma_A \Sigma_C \neq 0$ is one of the fix points on the global past attractor $\mathcal{A}_{\{**\}}$ for the Kasner subset \mathcal{K} given in equation (44).*

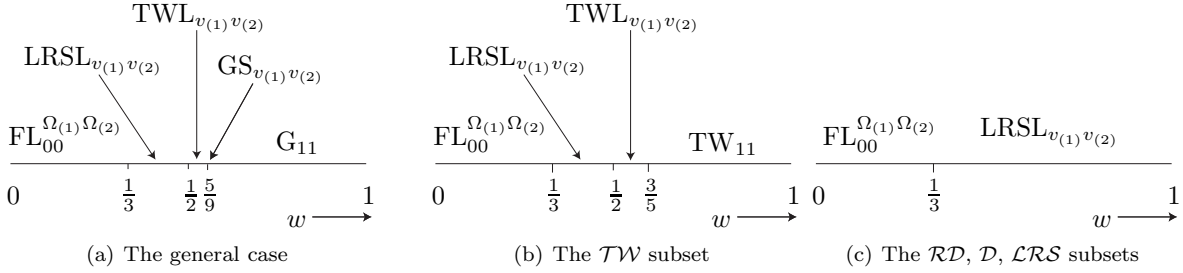


Figure 2: Future global attractor bifurcation diagrams for the various geometric subsets.

All of the tilted models approach a vacuum dominated Kasner singularity, where the influence of the matter becomes negligible. The fluids may either become aligned with each other and the normal congruence to the homogeneous hypersurfaces, or anti-aligned and extremely tilted, depending on the value of w and which of the Kasner states that is approached.

5 Summary and discussion

We have studied Bianchi type I models with two tilted fluids with the same linear equation of state, parameterized by the equation of state parameter w , using dynamical systems methods. The absence of spatial curvature in these models forces the fluids to be anti-aligned with each other. The paper was written with the modest ambition of completing the analysis of multi-fluid Bianchi type I models in [12] where it was assumed that one of the fluids were stiffer than the other (i.e. there were two different equations of state parameters such that $w_{(1)} > w_{(2)}$). As expected the models described here are in many ways similar to those in [12], and do, for example, exhibit rather similar bifurcation structure to the future, however, there are differences. One important difference is the existence of a constant of motion that correlates the velocities and energy densities of the fluids. This prohibits the asymptotic states to become single fluid cosmologies with an extra test field as was the case in many situations when the two fluids had different equations of state.

We proved that for models with $w = 0$ the system isotropizes to the future and approaches a future asymptotic Friedmann universe where both fluids become orthogonal to the homogenous hypersurfaces. For models with $w > 0$ we found equilibrium points that were future stable in the full state space and hence local future attractors. Numerical simulations indicate that these local attractors are also global future attractors, in the full state space and the invariant subspaces respectively. For equations of state softer than radiation the future attractors are the Friedmann points, corresponding to the self similar, isotropic Friedmann universe. A bifurcation occurs at the radiation value $w = 1/3$ where the future asymptotic state changes from a Friedmann universe to an anisotropic, but locally rotationally symmetric, state where both fluids acquire a non-zero tilt. There is a different fix point for each given value of a constant of motion, described in section 2.1. This result is different from the case when the case where one fluid is stiffer than the other, described in [12], where the stiffer fluid becomes extremely tilted. A second bifurcation occurs at $w = 1/2$ where the future asymptotic state acquires a second component of shear. Since the future asymptotic fix point is contained in the twisting subset, where $R_\alpha \neq 0$, $\phi = \text{const.}$, the asymptotic state is described relative to a constantly rotating frame. The frame is tied to the fluid three-velocity and hence indicates that the fluid is rotating relative to a Fermi frame. A final bifurcation occurs at $w = 5/9$ where the future asymptotic fix point is transferred from the twisting subset to the general anisotropic state space where $\Sigma_C \neq 0$. This implies that the decoupled variable ϕ is linearly decreasing ($\phi' = -\Sigma_C$) and hence that the frame rotation vector R_α is rotating in the plane spanned by \mathbf{e}_1 and \mathbf{e}_2 . Both fluid becomes extremely tilted (i.e. $|v_{(i)}| = 1$).

The past asymptotic state is for all non-self similar solutions a fix point located on the vacuum subset, generically either of zero or extreme tilt, depending on the asymptotic value of one of the shear variables. A subset of measure zero can asymptotically to the past have intermediate tilt if the shear variable Σ_+ tends to a specific value.

One can ask whether the anti-alignment of the fluids is a physically realistic scenario. Is there some mechanism which asymptotically would produce such a state from more general models? For past asymp-

otic behavior one could argue that there might be in many cases, since Bianchi type I models seem to be a part of the past attractor for very general cosmological models and for these models the fluids tend to become anti-aligned, but to really investigate whether this actually happens one must study two-fluid models in a more general context, one that at least contain Bianchi type II models.

A Fix points and local stability analysis

Kasner fix points: There are two circles of Kasner points and two surfaces of fix points when $0 \leq w$. The Kasner circles are characterized by $\Sigma_+ = \hat{\Sigma}_+$, $\Sigma_B = \hat{\Sigma}_-$, $\Sigma_A = \Sigma_C = 0$, $\Omega_{(1)} = \Omega_{(2)} = 0$, where $\hat{\Sigma}_\pm$ are constants that satisfy $\hat{\Sigma}_+^2 + \hat{\Sigma}_-^2 = 1$, and the following values of $v_{(i)}$:

$$K_{00}^\circ : v_{(1)} = v_{(2)} = 0, \quad K_{11}^\circ : v_{(1)} = -v_{(2)} = 1. \quad (26a)$$

The eigenvalues for the two cases are:

$$K_{00}^\circ : 0; \lambda_{\Sigma_A}; \lambda_{\Sigma_C}; \lambda_{v_{(1)}}^0; \lambda_{v_{(2)}}^0; 3(1-w); 3(1-w), \quad (27a)$$

$$K_{11}^\circ : 0; \lambda_{\Sigma_A}; \lambda_{\Sigma_C}; \lambda_{v_{(1)}}^1; \lambda_{v_{(2)}}^1; 2(1 + \hat{\Sigma}_+), \quad (27b)$$

where

$$\lambda_{\Sigma_A} = -(3\hat{\Sigma}_+ + \sqrt{3}\hat{\Sigma}_-), \quad \lambda_{\Sigma_C} = 2\sqrt{3}\hat{\Sigma}_-, \quad (28a)$$

$$\lambda_{v_{(i)}}^0 = 3w - 1 + 2\hat{\Sigma}_+, \quad \lambda_{v_{(i)}}^1 = -2(3w - 1 + 2\hat{\Sigma}_+)/(1 - w). \quad (28b)$$

In the K_{00}° case the Codazzi constraint (20b) is singular and hence it cannot be locally solved; in the other case (20b) has been used to eliminate $\Omega_{(1)}$. The zero eigenvalue corresponds to that one has a one-parameter set of fixed points. The two surfaces of Kasner fix points are characterized by

$$\begin{aligned} KS_{v_{(1)}v_{(2)}}^\pm : \quad \Sigma_A = \Sigma_C = \Omega_{(1)} = \Omega_{(2)} = 0, \quad \Sigma_+ = \frac{1}{2}(1 - 3w), \quad \Sigma_B = \pm\sqrt{1 - \Sigma_+^2}, \quad (29) \\ \left(\frac{v_{(1)}}{v_{(2)}}\right)^2 \cdot \left(\frac{1 - v_{(2)}^2}{1 - v_{(1)}^2}\right)^{(1-w)} = k. \end{aligned}$$

where the superscript denotes the sign of Σ_B , and k is the constant defined in (24). The relation between $v_{(1)}$, $v_{(2)}$ and k constrains the three free parameters and thus gives a surface of fix points. After eliminating $\Omega_{(1)}$ locally by means of the Codazzi constraint (20b), the eigenvalues for the Kasner surfaces are:

$$KS_{v_{(1)}v_{(2)}}^\pm : 0; 0; 0; \lambda_{\Sigma_A}; \lambda_{\Sigma_C}; 3(1 - w), \quad (30a)$$

where again $\lambda_{\Sigma_A} = -(3\hat{\Sigma}_+ + \sqrt{3}\hat{\Sigma}_-)$, $\lambda_{\Sigma_C} = 2\sqrt{3}\hat{\Sigma}_-$, where $\hat{\Sigma}_+$, $\hat{\Sigma}_-$ take the fix point values for the relevant line of fix points. Here two zero eigenvalues corresponds to that one has a surface of fix points while the third is associated with the existence of a one parameter set of solutions that are anti-parallel w.r.t. each other on each side of the surface of fix points.

Friedmann fix points: On the Friedmann subset there exists one line of fix points parameterized by the constant of motion k (24):

$$FL_{00}^{\Omega_{(1)}\Omega_{(2)}} : \Sigma_+ = \Sigma_A = \Sigma_B = \Sigma_C = 0, \quad \Omega_m = 1 \quad v_{(1)} = 0, \quad v_{(2)} = 0, \quad \frac{\Omega_{(1)}}{\Omega_{(2)}} = \sqrt{k}, \quad (31a)$$

where the superscript refers to the values of $\Omega_{(1)}$ and $\Omega_{(2)}$. The associated eigenvalues are:

$$FL_{00}^{\Omega_{(1)}\Omega_{(2)}} : \lambda_{1,2,3,4} = -\frac{3}{2}(1 - w); \quad 3w - 1; \quad 0, \quad (32a)$$

where we have used the Codazzi constraint (20b) to eliminate the variable $v_{(2)}$. Two of the eigenvalues of $\lambda_{1,2,3,4}$ refer to λ_{Σ_A} and λ_{Σ_C} .

Fix points on \mathcal{LRS} : When $\frac{1}{3} < w$ there is an additional line of fix points, $\text{LRSL}_{v_{(1)}v_{(2)}}$, which enter the physical state space when $w = \frac{1}{3}$, and move into the \mathcal{LRS} -subset with increasing values of w . The line intersects the foliation determined by (24) and can be parametrised by k . We have here chosen to use $v_{(1)}$ as a parameter instead for reasons of computational simplicity. In the stiff perfect fluid limit ($w = 1$) the line merge with the coalesced Kasner surfaces. The line of fix points is characterized by:

$$\begin{aligned} \text{LRSL}_{v_{(1)}v_{(2)}} : \\ \Sigma_A = \Sigma_B = \Sigma_C = 0, \quad \Sigma_+ = -\frac{1}{2}(3w-1), \quad v_{(2)}v_{(1)} = -\frac{3w-1}{5w+1}, \quad \frac{3w-1}{5w+1} \leq v_{(1)} \leq 1, \\ \Omega_{(1)} = \frac{3(1-w)(5w+1)(3w-1)(1+wv_{(1)}^2)}{4(1+w)[(5w+1)v_{(1)}^2 + (3w-1)]}, \quad \Omega_{(2)} = \frac{3(1-w)[(5w+1)^2v_{(1)}^2 + w(3w-1)^2]}{4(1+w)[(5w+1)v_{(1)}^2 + (3w-1)]}. \end{aligned} \quad (33a)$$

After eliminating $\Omega_{(1)}$ locally the eigenvalues for the LRS-line are:

$$\text{LRSL}_{v_{(1)}v_{(2)}} : \quad \lambda_{\Sigma_A} = 3(2w-1); \quad \lambda_{\Sigma_B} = \lambda_{\Sigma_C} = -\frac{3}{2}(1-w); \quad 0; \quad -\frac{3}{4}(1-w) \left(1 \pm \sqrt{A(w, v_{(1)})} \right), \quad (34a)$$

where $\text{Re } A(w, v_{(1)}) < 1$; since the expression for $A(w_{(i)})$ is rather messy we will refrain from giving it.

Fix points on \mathcal{TW} :

$$\text{TW}_{11} : \quad \Sigma_+ = -\frac{2}{5}, \quad \Sigma_C = 0, \quad \Sigma_A = \Sigma_B = \frac{\sqrt{3}}{5}, \quad v_{(1)} = 1, \quad v_{(2)} = -1, \quad \Omega_{(1)} = \Omega_{(2)} = \frac{3}{10}. \quad (35)$$

Local elimination of $\Omega_{(1)}$ by means of the Codazzi constraint (20b) yields the eigenvalues:

$$\lambda_{\Sigma_C} = \frac{3}{5}; \quad -\frac{3}{5}; \quad -\frac{3}{10}(1 \pm i\sqrt{39}); \quad \frac{6(3-5w)}{5(1-w)}; \quad \frac{6(3-5w)}{5(1-w)}. \quad (36)$$

When $\frac{1}{2} < w < \frac{3}{5}$ there exists one more line of fix points on \mathcal{TW} : $\text{TWL}_{v_{(1)}v_{(2)}}$. This line comes into existence when the line $\text{LRSL}_{v_{(1)}v_{(2)}}$ bifurcate into two at $w = \frac{1}{2}$; it then wanders away from \mathcal{D} when w increases and eventually leaves the physical state space through TW_{11} when $w = \frac{3}{5}$. Like $\text{LRSL}_{v_{(1)}v_{(2)}}$ it also can be parameterized by k but we choose $v_{(1)}$ here also for simplicity. The fix points are characterized by

$$\begin{aligned} \text{TWL}_{v_{(1)}v_{(2)}} : \quad \Sigma_+ = -\frac{1}{2}(3w_{(1)}-1), \quad \Sigma_A = \sqrt{\frac{3}{2}(1-w)(2w-1)}, \quad \Sigma_B = \sqrt{3}(2w-1), \\ \Sigma_C = 0, \quad v_{(1)}v_{(2)} = \frac{(1-w)(15w-7)}{-25w^2+18w-1}, \quad \frac{(1-w)(15w-7)}{-25w^2+18w-1} \leq v_{(1)} \leq 1, \\ \Omega_{(1)} = B(w, v_{(1)}), \quad \Omega_{(2)} = 1 - \frac{1}{4}(3w-1)(15w-7) - B(w, v_{(1)}), \end{aligned} \quad (37a)$$

where

$$B(w, v_{(1)}) = \frac{3}{4} \frac{(1-w)(7-15w)(25w^2-18w+1)(1+wv_{(1)}^2)}{(1+w)[(-25w^2+18w-1)v_{(1)}^2 + (1-w)(7-15w)]}. \quad (37b)$$

Local elimination of $\Omega_{(1)}$ yields the following eigenvalues:

$$\text{TWL}_{v_{(1)}v_{(2)}} : \quad \lambda_{\Sigma_C} = -\frac{3}{2}(5-9w); \quad 0; \quad \lambda_3(w, v_{(1)}); \quad \lambda_4(w, v_{(1)}); \quad \lambda_5(w, v_{(1)}); \quad \lambda_6(w, v_{(1)}), \quad (38a)$$

where $\lambda_{3,4,5,6}$ exhibit extremely messy expressions, which we therefore refrain from giving. They all have the property that the real part of the eigenvalues always are negative in the domain of definition of the fix point set, thus making the entire line a local attractor in the range $1/2 < w < 5/9$.

Fix point in the generic geometric manifold: There exists one fix point G_{11} for which all the off-diagonal components of the shear are non-zero. It thus exists on the generic ‘geometric’ manifold, but on the ‘matter boundary’ \mathcal{ET}_{11} where both fluids are extremely tilted. It is characterized by:

$$G_{11} : \quad \Sigma_+ = -\frac{1}{3}, \quad \Sigma_A = \frac{2}{3\sqrt{3}}, \quad \Sigma_B = \Sigma_C = \frac{1}{3\sqrt{3}}, \quad v_{(1)} = 1, \quad v_{(2)} = -1, \quad \Omega_{(1)} = \Omega_{(2)} = \frac{1}{3}. \quad (39)$$

Local elimination of $\Omega_{(1)}$ yields the eigenvalues:

$$\lambda_{1,2,3,4} = -\frac{1}{3} \left(1 \pm i\sqrt{23 \pm 12\sqrt{2}} \right); \quad \lambda_{5,6} = -\frac{2(9w-5)}{3(1-w)}. \quad (40)$$

At $w = \frac{5}{9}$ there exists a triangular surface of fix points, $\text{GS}_{v_{(1)}v_{(2)}}$, connecting $\text{TWL}_{v_{(1)}v_{(2)}}$ with G_{11} . $\text{GS}_{v_{(1)}v_{(2)}}$ is given by:

$$\begin{aligned} \text{GS}_{v_{(1)}v_{(2)}} : \quad \Sigma_+ &= -\frac{1}{3}, \quad \Sigma_A = \frac{\sqrt{2}}{3\sqrt{3}} \sqrt{\frac{17v_{(1)}v_{(2)}+3}{4v_{(1)}v_{(2)}-3}}, \quad \Sigma_B = \frac{1}{3\sqrt{3}}, \quad \Sigma_C = \frac{1}{3\sqrt{3}} \sqrt{\frac{13v_{(1)}v_{(2)}+6}{4v_{(1)}v_{(2)}-3}} \\ -1 &\leq v_{(1)}v_{(2)} \leq -\frac{6}{13}, \\ \Omega_{(1)} &= \frac{1}{3} \frac{-v_{(2)}(9+5v_{(1)}^2)}{(v_{(1)}-v_{(2)})(3-4v_{(1)}v_{(2)})}, \quad \Omega_{(2)} = \frac{1}{3} \frac{v_{(1)}(9+5v_{(2)}^2)}{(v_{(1)}-v_{(2)})(3-4v_{(1)}v_{(2)})}. \end{aligned} \quad (41a)$$

Local elimination of $\Omega_{(1)}$ yields two zero eigenvalues and four others with complicated dependence on $v_{(1)}$ and $v_{(2)}$ but which all have negative real part on the entire set $\text{GS}_{v_{(1)}v_{(2)}}$.

The local stability analysis of the fix points can be summarized in a table showing how the local attractor is transferred from set to set with increasing values of w - from the isotropic Friedmann solutions for sub-radiation equation of states to the increasingly anisotropic solutions when the fluid becomes stiffer.

invariant										
subset:	\mathcal{FLO}	\mathcal{LRS}		\mathcal{TW}		GENERIC MANIFOLD				
local										
sink:	$\text{FL}_{00}^{\Omega_{(1)}\Omega_{(2)}}$	\rightarrow	$\text{LRSL}_{v_{(1)}v_{(2)}}$	\rightarrow	$\text{TWL}_{v_{(1)}v_{(2)}}$	\rightarrow	$\text{GS}_{v_{(1)}v_{(2)}}$	\rightarrow	G_{11}	
w :	$\in [0, \frac{1}{3})$		$\in (\frac{1}{3}, \frac{1}{2}]$		$\in (\frac{1}{2}, \frac{5}{9})$		$\frac{5}{9}$		$\in (\frac{5}{9}, 1)$	

B The \mathcal{K} subset

We here discuss the Kasner subset \mathcal{K} with the state space $\mathbf{K} = \{\Sigma_+, \Sigma_A, \Sigma_B, \Sigma_C, v_{(1)}, v_{(2)}\}$, subjected to the constraints (20a) and (24). The equations for the test fields $v_{(1)} \in [0, 1]$, $v_{(2)} \in [-1, 0]$ decouple from those of the shear but are still coupled to each other through (24). The state space therefore can be written as the following Cartesian product:

$$\mathbf{K} = \mathbf{KP} \times \{v_{(1)}, v_{(2)}\}, \quad \mathbf{KP} = \{\Sigma_+, \Sigma_A, \Sigma_B, \Sigma_C\}, \quad (42)$$

where \mathbf{KP} is the projected Kasner state space, which of course is subjected to $\Sigma^2 = 1$. By determining the α - and ω -limits for solutions on \mathbf{KP} one can then determine the asymptotic states of $v_{(1)}$ and $v_{(2)}$, and thus the α - and ω -limits for solutions on \mathcal{K} . Let us therefore first turn to the equations on \mathbf{KP} :

$$\Sigma'_+ = 3\Sigma_A^2; \quad \Sigma'_A = -(3\Sigma_+ + \sqrt{3}\Sigma_B)\Sigma_A; \quad \Sigma'_B = \sqrt{3}\Sigma_A^2 - 2\sqrt{3}\Sigma_C^2; \quad \Sigma'_C = 2\sqrt{3}\Sigma_B\Sigma_C. \quad (43)$$

This system is defined on the compact space $\Sigma^2 = 1$. Since Σ_+ is monotonically increasing on a compact space it must approach a constant value, hence we have $\Sigma_A^2 \propto \Sigma'_+ \rightarrow 0$ asymptotically both to the future and to the past. Since we also have $(\Sigma_+ - \sqrt{3}\Sigma_B)' = -2\sqrt{3}\Sigma_C^2 \leq 0$, Σ_C will by the same argument also vanish asymptotically to both the future and to the past. $\Sigma_A = \Sigma_C = 0$ defines a circle of fix points, the projected Kasner circle: KP° , see Figure 3(a). It is described by $\Sigma_+ = \hat{\Sigma}_+$, $\Sigma_B = \hat{\Sigma}_-$, where the constants $\hat{\Sigma}_+$, $\hat{\Sigma}_-$ satisfy $\hat{\Sigma}_+^2 + \hat{\Sigma}_-^2 = 1$.

From this we conclude that the α -limits for all solutions with $\Sigma_A\Sigma_C \neq 0$ on \mathcal{KP} resides on the local source of KP° , yielding a segment on KP° characterized by $-1 \leq \Sigma_+ = \hat{\Sigma}_+ \leq -\frac{1}{2}$, $0 \leq \hat{\Sigma}_- \leq \frac{\sqrt{3}}{2}$, i.e., the segment consists of sector (213) together with the fix points Q_2 and T_3 on KP° . The ω -limit resides on the local sink, which consists of segment (312) together with the fix points Q_3 and T_2 , see Figure 3(b).

The α -limits for solutions on \mathcal{K} are determined by the α -limits on \mathcal{KP} which determine the asymptotic limits for $v_{(i)}$. The equation for $|v_{(i)}| \in [0, 1]$ on KP° is given by: $|v_{(i)}|' = (G_-^{(i)})^{-1}(1 - v_{(i)}^2)(3w - 1 +$

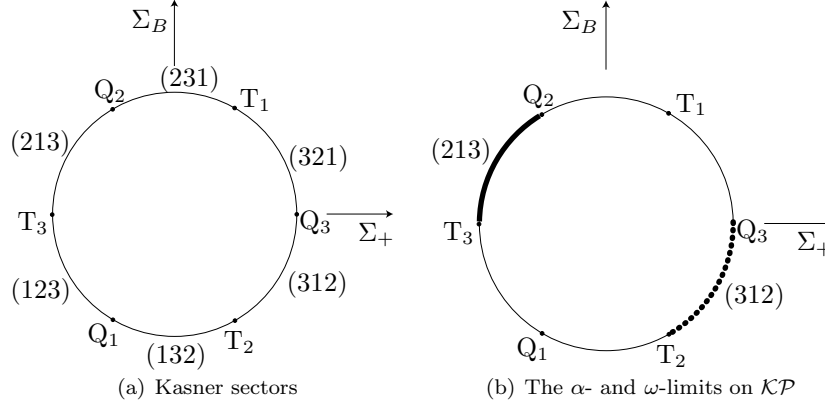


Figure 3: The projected Kasner circle KP° is divided into sectors (i, j, k) , defined by $\Sigma_i < \Sigma_j < \Sigma_k$, where i, j, k is a permutation of 1, 2, 3, and where $\Sigma_1 = \hat{\Sigma}_+ + \sqrt{3}\hat{\Sigma}_-$, $\Sigma_2 = \hat{\Sigma}_+ - \sqrt{3}\hat{\Sigma}_-$, $\Sigma_3 = -2\hat{\Sigma}_+$, and the points Q_α , corresponding to the non-flat plane symmetric Kasner solution, and T_α , corresponding to the Taub form for the Minkowski spacetime. The global past attractor for the general geometric set with $\Sigma_A \Sigma_B \neq 0$ on \mathcal{KP} consists of sector (213) together with Q_2 and T_3 on KP° . The global future attractor consists of sector (312) together with Q_3 and T_2 on KP° .

$2\hat{\Sigma}_+)|v_{(i)}|$. It follows that the α -limits for all orbits on \mathcal{K} on the general geometric set with $\Sigma_A \Sigma_C \neq 0$ resides on the global past attractor $\mathcal{A}_{\{**\}}$, where the subscript denotes the range of values of w , given by

$$\mathcal{A}_{\{w < \frac{2}{3}\}} = \{K_{11}^\circ : \hat{\Sigma}_+ \in [-1, -\frac{1}{2}]\}, \quad (44a)$$

$$\mathcal{A}_{\{w = \frac{2}{3}\}} = \{K_{11}^\circ : \hat{\Sigma}_+ \in [-1, -\frac{1}{2})\} \cup \{KS_{v_{(1)}v_{(2)}}^+ : \hat{\Sigma}_+ = -\frac{1}{2}\}, \quad (44b)$$

$$\mathcal{A}_{\{\frac{2}{3} < w\}} = \{K_{11}^\circ : \hat{\Sigma}_+ \in [-1, -\frac{1}{2}(3w-1))\} \cup \{KS_{v_{(1)}v_{(2)}}^+ : \hat{\Sigma}_+ = -\frac{1}{2}(3w-1)\} \cup \{K_{00}^\circ : \hat{\Sigma}_+ \in (-\frac{1}{2}(3w-1), -\frac{1}{2}]\}. \quad (44c)$$

The local stability analysis of the Kasner circle in the full Bianchi type I state space shows that the entire circle has unstable modes and will therefore not attract any orbits outside of the Kasner subset; the sinks on \mathcal{K} are saddle points in the full state space.

References

- [1] J. Wainwright and G. F. R. Ellis. *Dynamical systems in cosmology*, Cambridge: Cambridge University Press (1997).
- [2] C. G. Hewitt, R. Bridson, and J. Wainwright. The Asymptotic Regimes of Tilted Bianchi II Cosmologies. *Gen. Rel. Grav.* **33** 65 (2001).
- [3] J. D. Barrow and S. Hervik. The future of tilted Bianchi universes. *Class. Quantum Grav.* **20** 2841 (2003).
- [4] S. Hervik. The asymptotic behaviour of tilted Bianchi type VI_0 universes. *Class. Quantum Grav.* **21** 2301 (2004).
- [5] A. Coley and S. Hervik. A dynamical systems approach to the tilted Bianchi models of solvable type. *Class. Quantum Grav.* **22** 579 (2005).
- [6] S. Hervik, R. J. van den Hoogen, and A. Coley. Future asymptotic behaviour of tilted Bianchi models of type IV and VII_h . *Class. Quantum Grav.* **22** 607 (2005).

- [7] S. Hervik, R. J. van den Hoogen, W. C. Lim, and A. Coley. The futures of Bianchi type VII₀ cosmologies with vorticity. *Class. Quantum Grav.* **23** 845 (2006).
- [8] S. Hervik and W. C. Lim. The late time behaviour of vortic Bianchi type VIII universes. *Class. Quantum Grav.* **23** 3017 (2006).
- [9] S. Hervik, R. J. van den Hoogen, W. C. Lim, and A. Coley. Late-time behaviour of the tilted Bianchi type VI_h models. *Class. Quantum Grav.* **24** 3859 (2007).
- [10] S. Hervik, R. J. van den Hoogen, W. C. Lim, and A. Coley. Late-time behaviour of the tilted Bianchi type VI_{-1/9} models. *Class. Quantum Grav.* **25** 015002 (2008).
- [11] A. Coley and S. Hervik. Bianchi models with vorticity: The type III bifurcation. arXiv.0802.3629v1.
- [12] P. Sandin and C. Uggla. Bianchi type I models with two tilted fluids. arXiv:0806.0759.
- [13] C. Uggla,, H. van Elst, J. Wainwright and G. F. R. Ellis. The past attractor in inhomogeneous cosmology. *Phys. Rev. D* **68** : 103502 (2003).
- [14] G. F. R. Ellis and H. van Elst. Cosmological models (Cargèse lectures 1998) in *Theoretical and Observational Cosmology*, edited by M. Lachièze-Rey, Dordrecht: Kluwer (1999) p. 1.
- [15] V. G. LeBlanc. Asymptotic states of magnetic Bianchi I cosmologies. *Class. Quantum Grav.* **14** 2281 (1997).
- [16] J. A. Tyson, F. Valdes and R. A. Wenk. Detection of systematic gravitational lens galaxy image alignments: Mapping dark matter in galaxy clusters. *Astrophys. J.* 349, L1 (1990).